Acta Pharmaceutica Sinica B 2026;16(1):239−251

Chinese Pharmaceutical Association
Institute of Materia Medica, Chinese Academy of Medical Sciences

Acta Pharmaceutica Sinica B

www.elsevier.com/locate/apsb
www.sciencedirect.com

ORIGINAL ARTICLE

Attenuated *Salmonella* secreting interleukin-21 activates T-cells and induces anti-tumor effects

Minju Han[a], Eunji Kim[a], Minchan Jeong[a], Solbi Kim[b], Hyo-Jin Lee[a,b,c,*], Heung Jin Jeon[b,*]

[a]*Department of Medical Science, College of Medicine, Chungnam National University, Daejeon 34134, Republic of Korea*
[b]*Cancer Research Institute, Chungnam National University, Daejeon 34134, Republic of Korea*
[c]*Division of Hemato-Oncology, Department of Internal Medicine, Chungnam National University Hospital, Daejeon 35015, Republic of Korea*

Received 30 April 2025; received in revised form 24 July 2025; accepted 11 August 2025

KEY WORDS

Engineering *Salmonella*;
Interleukin-21;
Immunotherapy;
Immune checkpoint inhibitor;
Flagellar type-3 secretion system;
Tumor microenvironment;
Combination therapy;
Anti-tumor effect

Abstract The tumor microenvironment is characterized by an immunosuppressive state. Although PD-1/PD-L1 blockade therapy activates the immune system against tumors, it has limited long-term efficacy, prompting the development of combination therapies with targeted treatments to improve cancer treatment outcomes. Recent advancements have revitalized interest in using attenuated *Salmonella* strains as cancer therapeutics that target tumors, induce immune responses, and promote tumor cell death, although complete tumor suppression remains challenging. We aimed to induce antitumor effects by activating the suppressed immune system within the tumor microenvironment using *Salmonella*-mediated secretion of interleukin-21 (IL-21). We used the tumor-targeting ability of *Salmonella* and its flagellar type-3 secretion system (FT3SS) to induce the secretion of IL-21 into the tumor microenvironment *via* the flagellar system and evaluated the local immune response. We also evaluated the efficacy of combining *Salmonella*-mediated IL-21 delivery and anti-PD-L1 therapy in a mouse model. IL-21 secretion promoted the recruitment of $CD4^+$ and $CD8^+$ T cells and enhanced the expression of cytotoxicity-related molecules. Tumor-bearing mice treated with the combination therapy with anti-PD-L1 antibodies showed improved survival rates and enhanced tumor growth inhibition. This study demonstrates the tumor-targeting capability and *in vivo* safety of *Salmonella*, highlighting its potential as a powerful cancer therapy platform.

*Corresponding authors.
E-mail addresses: cymed@cnu.ac.kr (Hyo-Jin Lee), livinglogos@cnu.ac.kr (Heung Jin Jeon).

Peer review under the responsibility of Chinese Pharmaceutical Association and Institute of Materia Medica, Chinese Academy of Medical Sciences.

https://doi.org/10.1016/j.apsb.2025.09.025

1. Introduction

Various strategies are being explored to overcome the limitations of traditional cancer treatments such as surgery, chemotherapy, and radiation therapy[1,2]. Immunotherapy offers an innovative approach to target cancer cells by modulating the immune system, and its scope expands as research progresses[3]. Tumors often exploit immune suppression pathways to evade tumor antigen-specific T cells, and immune checkpoints (ICs) are frequently upregulated in the tumor microenvironment (TME) of various cancers[4]. Programmed cell death ligand 1 (PD-L1) is expressed on tumor cells and binds to programmed cell death protein 1 (PD-1) on T cells, suppressing immune responses and enabling tumor immune evasion[5]. PD-1/PD-L1 blockade therapy has shown remarkable success in activating the immune system in the TME[6]. However, only 10%−30% of patients treated with PD-1/PD-L1 inhibitors experience long-term efficacy[7]. To improve response rates, combination therapies that combine immunotherapy with targeted treatments are being developed for more effective cancer treatment[1]. Combining immune checkpoint inhibitors with therapies such as surgery and radiation, is expected to significantly enhance treatment outcomes[8].

The potential use of bacteria as cancer therapeutics has long been recognized. Bacteria, such as *Salmonella*, target solid tumors through unique mechanisms, including preferential accumulation in hypoxic and immunosuppressive tumor microenvironments, active migration toward tumor-associated chemoattractants, and immune evasion strategies. *Salmonella* selectively thrives in tumor microenvironments rich in specific metabolites, such as lactate and necrotic debris, and promotes tumor cell death through direct bacterial toxicity, competition for nutrients, and the induction of immune responses[1]. While chemotherapy and radiation have led to a decline in bacterial-based cancer research, recent developments have revitalized the interest in this approach[9-13]. An attenuated *Salmonella* strain has been developed by deleting virulence genes, reducing toxicity, while maintaining antitumor efficacy, and has proven safe in clinical trials. Additionally, *Salmonella* pathogenicity enhances antitumor effects by inducing a host immune response and increasing $CD8^+$ and $CD4^+$ T cells[14-16]. However, achieving complete tumor suppression using *Salmonella* alone remains a challenge.

To enhance bacterial-based cancer therapy, research has focused on using expression systems to deliver therapeutic agents such as cytotoxic substances, immune modulators, and small interfering RNA[17,18]. Among the seven bacterial secretion systems, type-3 secretion system (T3SS) can be engineered to deliver anticancer proteins. For instance, FlgM in flagellar T3SS can be modified to secrete anticancer proteins while reducing bacterial motility, keeping the bacteria localized within the tumor[19-21]. This approach further underscores the potential of engineered bacteria in cancer therapy.

Interleukin-21 (IL-21) plays a crucial role in cancer immunotherapy by regulating and activating immune cells. IL-21, secreted by activated helper T-cells, binds to the IL-21 receptor (IL-21R), which includes the IL-21Rα chain (RA) and IL-2RγC common chain. IL-21 stimulates IFN-γ production and enhances cytotoxic activity of natural killer (NK) and $CD8^+$ T cells. Through these processes, IL-21 boosts the function of cytotoxic T cells and NK cells, thereby promoting antitumor immune responses and enhancing the activation of the immune system against cancer[18,22-25] Additionally, the antitumor effects of IL-21 can be further enhanced when combined with other immunotherapies, such as anti-PD-1 or anti-PD-L1 treatments[26]. Such combination therapies leverage the immunoregulatory properties of IL-21 to induce a more effective immune response against tumors.

In this study, we developed a modified *Salmonella* strain that secretes IL-21 by using FT3SS. FlgM-tagged IL-21 was secreted under the control of the P_{BAD} promoter in the presence of L-arabinose. The successful secretion of IL-21 by the modified *Salmonella* strain was confirmed, demonstrating the functional viability of the strain. Additionally, in tumor-bearing mouse models, this strain induces the recruitment of $CD4^+$ and $CD8^+$ T cells into the tumor microenvironment, demonstrating notable antitumor effects, particularly through the activation of IFN-γ, perforin, and granzyme B secreted by $CD8^+$ T cells, thereby validating its potential to enhance immune responses against tumors. Combination therapy with an anti-PD-L1 antibody significantly increased antitumor effects and substantially improved survival rates. This study demonstrates the safety of *Salmonella* strains secreting IL-21 and highlights the strong potential of engineered *Salmonella* strains as anticancer agents.

2. Materials and methods

2.1. Bacterial strains

Salmonella strain *BRD509* (*aroA aroD− Salmonella*, a mutant of *SL1344*)[27] was utilized to generate a strain with deletions in the *asd* and *rcsB* genes (*aroA aroD asd rcsB− SL1344*) (Supporting Information Table S1). Both *BRD509* and *BRD509 asd−* strains were obtained from Professor In Soo Lee at Hannam University, Republic of Korea. The *rcsB* gene was deleted using the lambda-mediated targeted mutagenesis method[28] with the primers *rcsB*-pkd13-For and *rcsB*-pkd13-Re, resulting in the creation of the *aroA aroD rcsB− Salmonella* strain (#245) (Supporting Information Tables S1 and S2). Subsequently, P22 phage (strain construction utilizing P22-mediated generalized transduction)[29] was employed to transduce strain #245 into the *BRD509 asd−* (#177) strain, thereby constructing strain #1237 (Table S1). This strain was confirmed to contain the flgM-mIL-21 plasmid and was designated as flgM-mIL-21-flhDC-pBAD18-asd+/#1237 (*aroA aroD asd rcsB−*), and ultimately finalized as strain #1550 (Table S1). To facilitate the *in vivo* imaging system (IVIS) analysis, we transformed the pGEN-luxCDABE plasmid into strain #1237, creating strain #2487. pGEN-luxCDABE was a gift from Harry Mobley (Addgene plasmid # 44918; http://n2t.net/addgene:44918; RRID: Addgene_44918)[30]. The flgM-mIL-21 plasmid was introduced into strain #2487 to generate strain #2526. All DNA manipulations were performed using the *Escherichia coli* strain

DH5α. The plasmids were transferred into *S. typhimurium SF586* (#46) *via* electroporation, followed by transformation into the corresponding strains.

2.2. Plasmid construction for IL-21 secretion

FlgM protein and mIL-21 were translation-fused to design FlgM-mIL-21, with FlgM and mIL-21 connected *via* an 8 × His tag (Supporting Information Fig. S1A)[19]. Subsequently, this construct was converted into DNA and codon-optimized (Fig. S1B and S1C). flgM-His-mIL-21 DNA was synthesized by Cosmogenetech (Seoul, Korea). The P_{BAD} vector containing an arabinose induction system was used[31,32]. A plasmid encoding recombinant mIL-21 was constructed by ligating a DNA fragment encoding flgM-mIL-21 with pBAD18, after digestion with NheI (#1241A; Takara Bio Inc., Shiga, Japan) and SacI (#1078A; Takara Bio Inc., Shiga, Japan). The resulting plasmid was named as flgM-mIL-21. Using flhD-Sac1-for and flhC-Sal1-re primers, PCR was performed using LT2 *Salmonella* as the template. The resulting product was ligated into the flgM-mIL-21 construct by enzyme digestion, and *flhDC* was inserted behind flgM-mIL-21 (Table S1). The coding sequences of *flhDC* and RBS were cloned into flgM-mIL-21 following SacI and SalI (#1080A, Takara Bio Inc., Shiga, Japan) digestion. To insert the *asd* gene, the previously constructed plasmid was digested with ClaI (#1034A, Takara Bio Inc., Shiga, Japan), and a PCR fragment was amplified using asd-ClaI-For and asd-ClaI-RE primers with LT2 *Salmonella* as the template, which was also digested with ClaI. The two fragments were ligated to complete the flgM-mIL-21-flhDC-pBad18-asd + plasmid (Fig. 1A)[33].

2.3. Western blot analysis

After overnight cultivation of the *Salmonella* strain secreting IL-21, the culture was incubated at 37 °C for 1 h with shaking at 250 rpm in LB broth containing 100 μg/mL ampicillin. When the OD at 600 nm reached 0.2, L-arabinose was added to a final concentration of 0.2%, and the culture was incubated at 170 rpm for 6 h. To confirm that the secreted protein was IL-21, whole cells, cell lysates, and supernatants were collected from the culture media. Whole cells, cell lysates, and supernatants were separated by 12% sodium dodecyl sulfate-polyacrylamide gel electrophoresis (SDS-PAGE), and the separated proteins were analyzed by Western blotting. During *Salmonella* cultivation, supernatants were collected at various time points under L-arabinose induction to monitor the increase in IL-21 levels, which were analyzed using Western blotting. IL-21 was detected using an anti-His antibody (#SB194b, SouthernBiotech, AL, USA) or anti-mIL-21 antibody (#MAB594, R&D Systems, Minneapolis, MN, USA). The secondary antibodies used were HRP-conjugated anti-mIgG (#7076, Cell Signaling Technology, Danvers, MA, USA) or anti-rat IgG (#AB97057, Abcam, Cambridge, UK).

2.4. ELISA assay

The secretion efficiency of IL-21 was measured by ELISA. *Salmonella* secreting IL-21 (500 μL) was inoculated into 50 mL of resistant LB medium and cultured until the OD_{600} reached 0.4−0.6. Subsequently, 20% L-arabinose was added to induce protein expression at 37 °C. The bacterial culture was then collected and bacteria were removed using a 0.22 μm filter. The induced supernatant was stored at −80 °C.

Additionally, *Salmonella*-secreting IL-21 (2×10^7 CFU) was intravenously injected, and the tumors were harvested on Day 7 post-injection. The tumors were homogenized using a Tissue Lyser, and the supernatant was stored at −80 °C. After collecting all supernatant samples, the IL-21 concentration was measured using a mouse IL-21 ELISA Kit (KE10012, Proteintech, Rosemont, IL, USA).

2.5. Bacterial growth assay

After culturing IL-21-secreting *Salmonella* in a shaking flask at 37 °C and 250 rpm, 0.2% L-arabinose was added when the OD_{600} reached 0.2, and the culture was incubated for 1 day at 37 °C. The absorbance of the culture was measured at 600 nm every hour using a spectrophotometer.

2.6. Animals and tumor models

6−7 weeks old female BALB/c mice were purchased from NARA Biotech (South Korea), and the mice ($n = 5$/group) were housed in ventilated cages, maintaining a constant room temperature at the Preclinical Research Center of Chungnam National University Hospital. All animal experiments were approved by the Institutional Animal Care and Use Committee (IACUC) of Chungnam National University and were conducted in compliance with the guidelines (CNUH-2023-IA0095-00). A subcutaneous tumor model was established by injecting 5×10^5 CT26 cells (suspended in 30 μL of PBS) into the right flank of BALB/c mice. When the average tumor size reached approximately 100−150 mm^3, the mice were divided into various groups and treated intravenously with 2×10^7 CFU of *Salmonella* strains or *Salmonella* strains secreting IL-21. The secretion of IL-21 was induced by daily intraperitoneal administration of L-arabinose (80 mg/mouse) starting 3 days post-infection (dpi). To evaluate the effects of the combination therapy, an anti-PD-L1 antibody (200 μg/mouse; Bio X cell, Lebanon, NH, USA) was administered intraperitoneally on Days 0, 3, 6, and 9. The mice were monitored twice weekly for tumor volume, weight, and survival rate. Each tumor was measured every two days using digital calipers, and the tumor volume (mm^3) was calculated using Eq. (1):

$$\text{Tumor volume} = (a \times b^2) \times 1/2 \quad (1)$$

where a is the width at the widest point of the tumor and b is the width perpendicular to a. The mice were euthanized when the tumor volume reached 1500 mm^3.

2.7. Flow cytometry analysis

Tumors were collected on 7 dpi for flow cytometry analysis. Tumor samples were weighed, cut into approximately 1 mm^3 pieces, and 0.5 g of tissue was digested in 5 mL of digestion solution [RPMI 1640 containing collagenase type IV (1.0 mg/mL) and DNase I (50 μg/mL)] at 37 °C for 30 min using a water bath shaker.

The samples were then passed through a 40 μm nylon mesh filter to obtain a single-cell suspension. The following antibodies were used to analyze activated T-cells: anti-CD3-PE-eF610 (61-0031-82, eBioscience, San Diego, CA, USA), anti-CD4-PerCP (46-0041-82, eBioscience, San Diego, CA, USA), anti-CD8-AF700 (56-0081-82, eBioscience, San Diego, CA, USA), and anti-FVD-APC-Cy7 (65-0865-14, eBioscience, San

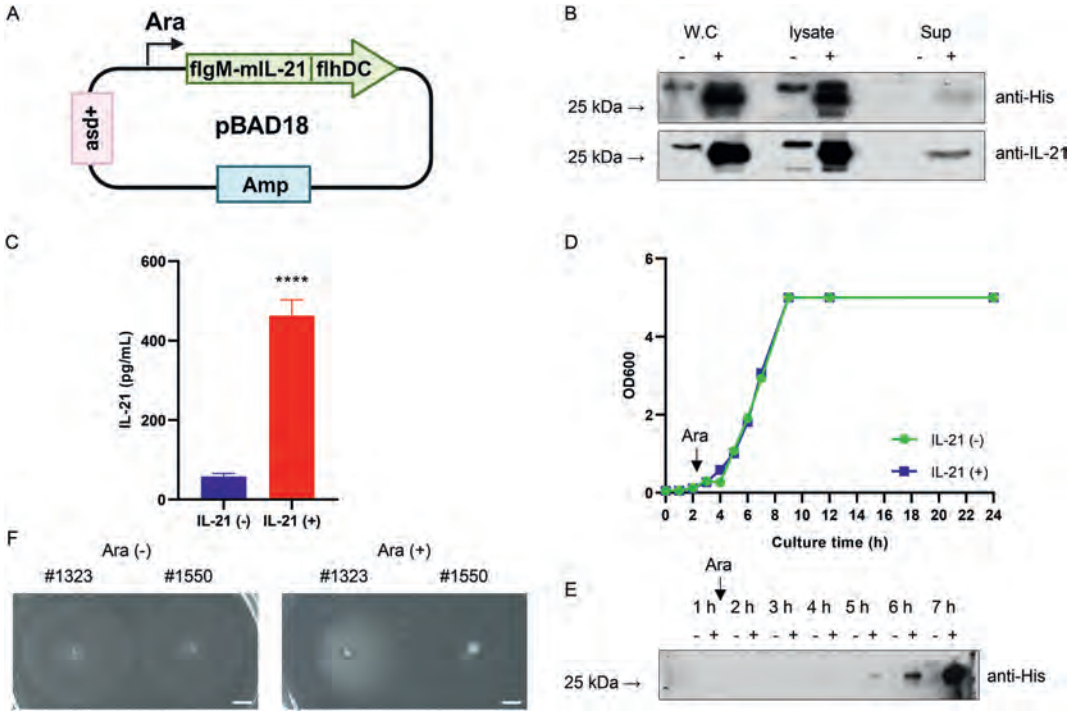

Figure 1 Construction and characterization of IL-21-secreting *Salmonella*. (A) Plasmid map designed for the secretion of FlgM-tagged IL-21. (B) After overnight culturing of the *Salmonella* strain secreting IL-21, 0.2% L-arabinose was added to induce IL-21 expression. Whole cells, cell lysates, and supernatants were collected, and Western blot analysis was performed using anti-His and anti-IL-21 antibodies, respectively. (C) IL-21 secretion was confirmed by ELISA ($n = 5$). (D) Growth of the strain secreting IL-21 was compared between induced (0.2% L-arabinose) and non-induced groups by measuring the OD at 600 nm. (E) Western blot analysis using anti-His was conducted to track the secretion of IL-21 over time following induction with 0.2% L-arabinose. (F) Motility assays were performed to examine the motility of the IL-21-secreting strain under 0.2% L-arabinose. The experiments were repeated at least three times, and representative data are shown. Scale bar = 5 mm. Significance is indicated as $****P < 0.0001$. Data are presented as mean ± SEM.

Diego, CA, USA). Fluorescent signals were measured using a flow cytometer (BD Biosciences, Franklin Lakes, NJ, USA) and the data were analyzed using FlowJo software (TreeStar, Ashland, OR, USA).

2.8. *Immunohistochemistry and immunofluorescent analysis*

Tumor tissues from each group were collected at 21 dpi and embedded in 4-μm thick paraffin sections for immunohistochemistry (IHC) staining. The sections were stained with hematoxylin and eosin (H&E). Tumor sections were stained using terminal deoxynucleotidyl transferase dUTP nick-end labeling (TUNEL) to detect apoptosis, and Ki-67 immunohistochemistry was performed to assess cell proliferation. Apoptotic cells were identified using the TUNEL Assay Kit-HRP-DAB (#AB206386, Abcam, Cambridge, UK). For Ki-67 staining, the slides were incubated overnight at 4 °C in a humid chamber with anti-Ki-67 antibody (#12202, Cell Signaling Technology, Danvers, MA, USA). The diaminobenzidine (DAB) detection system (K3468, Dako, Glostrup, Denmark) was used for visualization, following the manufacturer's instructions. For immunofluorescence (IF) staining, tumors were collected at 7 dpi and slices were prepared using cryoblocks to verify the presence of $CD4^+$ and $CD8^+$ T cells within the tissue sections. Additionally, cytotoxic T cells were analyzed for granzyme B, perforin, and IFN-γ using IF methods. The antibodies used for immunofluorescence included anti-CD4 (#183685, Abcam, Cambridge, UK), anti-CD8α (#AB22378, Abcam, Cambridge, UK), anti-IFN-γ (#133566, Abcam, Cambridge, UK), anti-granzyme B (#17215S, Cell Signaling Technology, Danvers, MA, USA), anti-perforin (#44865S, Cell Signaling Technology, Danvers, MA, USA), and anti-PD-L1 (#AB213480, abcam, Cambridge, UK). All the samples were analyzed using a confocal microscope (Zeiss, Oberkochen, Germany).

2.9. *In vivo biodistribution*

To study the tumor-targeting ability and safety of *Salmonella*, mice with tumor volumes of 100−150 mm^3 were intravenously injected with 2×10^7 CFU #2487 (Table S2). Subsequently, the mice were subjected to *in vivo* fluorescence imaging using an IVIS system to obtain fluorescence images 2, 24, 48, 168, and 336 h after injection. Additionally, mice were sacrificed at each time point, and tissues, including the tumors, heart, liver, spleen, lungs, and kidneys, were collected to measure the fluorescence intensity.

2.10. *Agar plate count assay*

To quantify the *in vivo* distribution and bacterial load within the tumors, mice with tumor volumes of 100−150 mm^3 were intravenously injected with 2×10^7 CFU of *Salmonella*. Subsequently, tumors and major organs, such as the heart, liver, spleen, lungs, and kidneys, were collected at 1, 7, and 14 dpi, weighed, and homogenized in phosphate-buffered saline (PBS). The samples

were then plated on LB agar containing 100 μg/mL ampicillin and incubated overnight at 37 °C. After incubation, bacterial colonies were counted.

2.11. Safety evaluation

After intravenous injection of 2×10^7 CFU of *Salmonella,* blood samples were collected from each group on Days 7, 14, and 21 and centrifuged at 5095 × *g* for 10 min at 4 °C to obtain serum. Serum biochemical marker levels, including alanine aminotransferase (ALT), aspartate aminotransferase (AST), blood urea nitrogen (BUN), and creatinine (CREA), were measured using the respective analysis kits.

2.12. Statistical analysis

The experimental results are presented as mean ± standard error of the mean (SEM). Statistical significance was determined using GraphPad Prism version 8.0 (GraphPad Software). Statistical differences between the two groups were determined using a two-tailed Student's *t*-test or Mann−Whitney U test. *P*-values less than 0.05 were considered significant and denoted as $*P < 0.05$, $**P < 0.01$, $***P < 0.001$, $****P < 0.0001$; ns = not significant.

3. Results

3.1. Construction and characterization of Salmonella secreting IL-21

Salmonella was transformed with a P_{BAD} plasmid engineered to express IL-21 (Table S2). This plasmid contained the *IL21* gene tagged with FlgM, *flhDC*, and *asd* (Fig. 1A). Following induction with L-arabinose, IL-21 protein secretion was measured in both the cell lysate and the supernatant, revealing the expression of a protein with an approximate molecular weight of 25 kDa. This was confirmed by Western blotting with anti-His and anti-IL-21 antibodies (Fig. 1B). IL-21 secretion was confirmed by ELISA following L-arabinose induction (Fig. 1C). Evaluation of the growth of *Salmonella* with and without L-arabinose (0.2%) showed that L-arabinose did not affect growth (Fig. 1D). Additionally, Western blot analysis demonstrated that IL-21 secretion increased over time after L-arabinose treatment (Fig. 1E). Using a motility assay, we confirmed that the motility of IL-21-secreting *Salmonella* decreased as fliC expression decreased with the addition of L-arabinose (Fig. 1F). These results indicate that IL-21 was successfully secreted following L-arabinose induction.

3.2. Antitumor efficacy of Salmonella secreting IL-21 in tumor-bearing mice

After intravenous administration of the *Salmonella* strain, IL-21 secretion was induced by intraperitoneal injection of L-arabinose starting on Day 3 (Fig. 2A). Tumor size, body weight, and survival rate were monitored periodically. On Day 2, the tumor sizes were similar across all groups. However, after *Salmonella* administration, tumor size gradually decreased, with more pronounced reductions observed following L-arabinose induction (Fig. 2B and C). The tumor growth data for each group are shown in Supporting Information Fig. S2. Additionally, a *Salmonella* strain secreting FlgM alone was generated to evaluate the effect of FlgM on tumor growth (Supporting Information Fig. S3). The results showed that *Salmonella*-secreting FlgM did not demonstrate significant tumor growth inhibition compared with the IL-21-secreting strain. These findings strongly suggest that IL-21 directly contributes to tumor suppression, whereas FlgM does not. The body weights of mice treated with *Salmonella* recovered within five days and remained stable throughout the treatment period, indicating the safety of live *Salmonella* administration (Fig. 2D). Based on the antitumor effects mediated by IL-21 secretion, on Day 15, when the tumor size reached 1500 mm^3, the L-arabinose induction group showed a 70% increase in survival rate compared to the PBS group and a 57.14% increase in survival rate compared to the *Salmonella* alone group and the group without L-arabinose induction (Fig. 2E). Tumor tissues collected from each group on Day 21 showed increased cell death, as determined by TUNEL assay, and a significant decrease in Ki-67 expression (Fig. 2F−I).

3.3. IL-21-secreting Salmonella promotes T cell infiltration and antitumor activity

The antitumor effects of IL-21 secreted by *Salmonella* were evaluated in tumor-bearing mice. In this study, tumors from mice treated with various therapies were harvested on Day 7, and single-cell suspensions were prepared for flow cytometry analysis to detect IL-21 and analyze tumor-infiltrating immune cells (Fig. 3A). IL-21 secretion was assessed by measuring the IL-21 concentration in tumor samples using ELISA. IL-21 was not detected in the PBS, *Salmonella*-only, or *Salmonella* groups without IL-21 secretion, whereas it was measured at 147 pg/mL in the L-arabinose-induced group (Fig. 3B). IL-21 secretion was confirmed by using anti-IL-21 and anti-His antibodies (Supporting Information Fig. S4). In the L-arabinose-treated group, IL-21 secretion was confirmed by IHC staining and IF analysis (Fig. 3C and D). IL-21 plays a crucial role in immune responses, promoting the activation and proliferation of $CD4^+$ and $CD8^+$ T cells, and particularly enhancing the cytotoxicity of $CD8^+$ T cells to attack tumors and infected cells. As shown in Fig. 3E−G, L-arabinose-induced IL-21 increased the proportion of $CD4^+$ and $CD8^+$ T cells in tumor cells. These findings confirmed that IL-21 activates a potent immune response that promotes tumor clearance and enhances antitumor immune responses.

Additionally, the activation of immune cells induced by IL-21 secretion was confirmed using IHC staining and IF analysis. IHC analysis showed a significant increase in the infiltration of $CD4^+$ and $CD8^+$ T cells in the L-arabinose-induced group compared to that in the other groups (Supporting Information Fig. S5). These results were confirmed by the IF analysis (Fig. 4A and B). Moreover, the expression of cytotoxic molecules such as granzyme B and perforin was significantly elevated in $CD8^+$ T cells in the L-arabinose-induced group (Fig. 4C and D). In addition, IFN-γ was also detected (Supporting Information Fig. S6). The quantitative IF analysis results are presented in Fig. 4E−H. These findings suggest that IL-21 secreted by *Salmonella* enhances the immune response within tumors by activating $CD4^+$ and $CD8^+$ T cells.

3.4. Antitumor efficacy of Salmonella secreting IL-21 combined with anti-PD-L1 antibody in tumor-bearing mice

The TME is generally less immunogenic than normal tissues, making it challenging to respond to ICI and limit the activation of cytotoxic T cells[34]. To enhance the immune response by

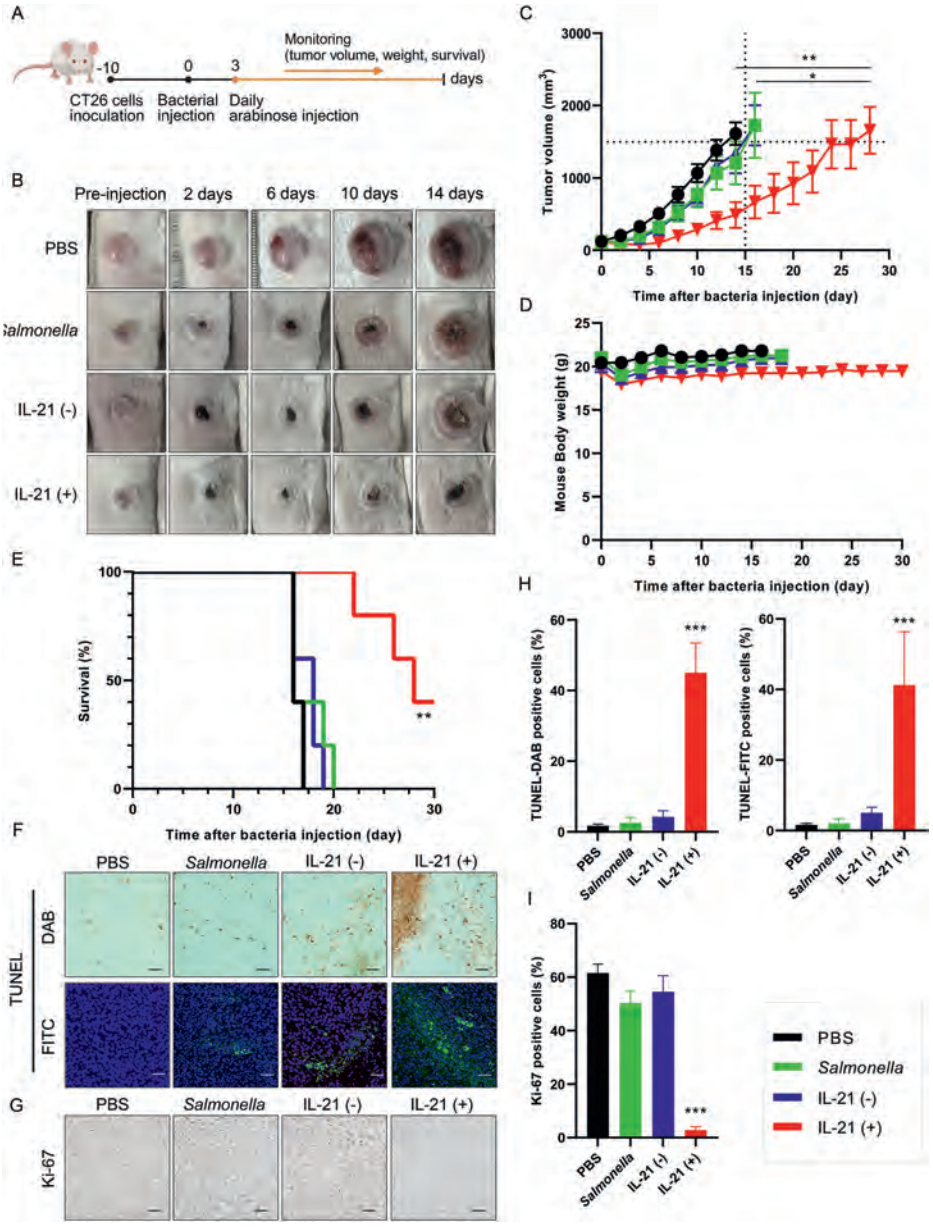

Figure 2 Antitumor efficacy of IL-21-secreting *Salmonella* in tumor-bearing mice. (A) Treatment schedule for cancer therapy using IL-21-secreting *Salmonella*. CT26 cells (5×10^5) were subcutaneously injected into the right flank of BALB/c mice. When the tumor size reached approximately 100 mm^3, *Salmonella* (2×10^7 CFU) was administered intravenously, and from Day 3 post-injection, L-arabinose (80 mg/mouse) was administered intraperitoneally. IL-21(−), without L-arabinose; IL-21(+), with L-arabinose. (B) Representative images of tumor-bearing mice. (C) Tumor volume at 2-day intervals. (D) Body weight changes in each treatment group. (E) Survival curves for each treatment group (data from B−E; $n = 7$). (F) TUNEL analysis of tumors from each treatment group. (G) Ki-67 expression in tumors from each treatment group. bar = 50 μm. Image quantification data are presented in (H, I) (data from F−I; $n = 3$). Significance is indicated as $^*P < 0.05$, $^{**}P < 0.01$, $^{***}P < 0.001$. Data are presented as the mean ± SEM.

combining IL-21 with anti-PD-L1 antibodies, *Salmonella* was used to regulate PD-L1 expression in the TME. PD-L1 expression in tumor cells increased over time (24, 48, 72, and 96 h) after the bacterial injection (Supporting Information Fig. S7). Anti-PD-L1 was administered intraperitoneally at four different time points (0, 3, 6, and 9 days) and L-arabinose was administered from 3 dpi to induce IL-21 secretion (Fig. 5A). All experimental groups had similar tumor sizes at 2 dpi; however, the group treated with both L-arabinose and anti-PD-L1 showed a more significant antitumor effect than that treated with L-arabinose alone. Notably, 40% of the mice in the combination therapy group (two of five) showed complete tumor regression (Fig. 5B and C). The growth curves of individual tumors in each group are shown in Supporting Information Fig. S8. The weights of mice treated with *Salmonella* recovered within five days and remained stable throughout the treatment period, indicating the safety of live *Salmonella* administration (Fig. 5D). Survival rates improved in the group that received both L-arabinose and anti-PD-L1 therapy compared with

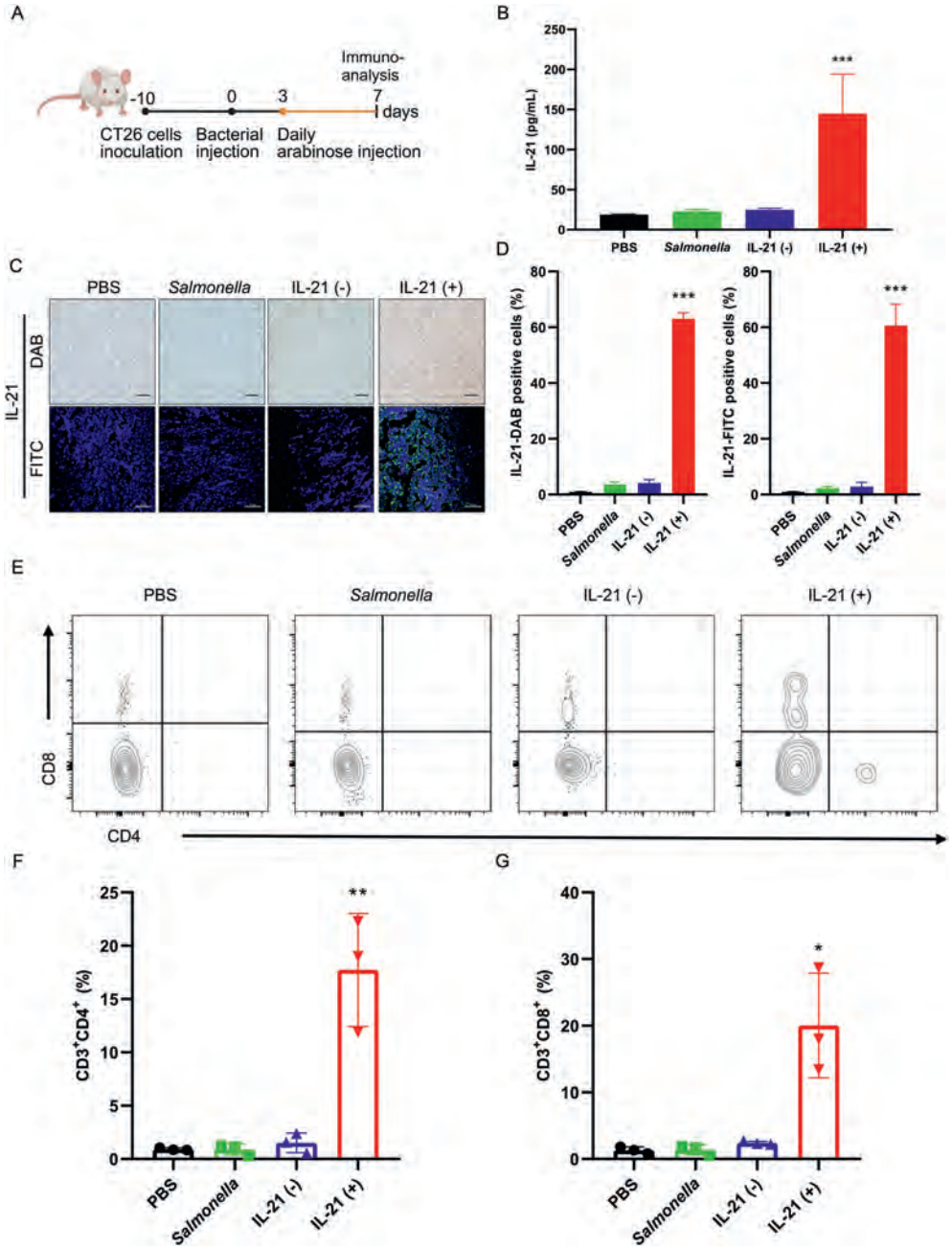

Figure 3 IL-21-secreting *Salmonella* promotes T cell infiltration and antitumor activity. (A) Experimental scheme in tumor-bearing mice: Immune cells were analyzed in tumor tissues on Day 7. (B) Anti-IL-21 was detected in the tumor tissues using ELISA. (C) In tumor tissues, anti-IL-21 was confirmed through IHC. Scale bar = 50 μm. (D) Image quantification data (data from B−D; $n = 3$). (E−G) Flow cytometry analysis showed that $CD4^+$ and $CD8^+$ T cells were activated by IL-21 in mouse tumor tissues (data from E−G; $n = 3$). Significance is indicated as $^*P < 0.05$, $^{**}P < 0.01$, $^{***}P < 0.001$. Data are presented as the mean ± SEM.

those that received L-arabinose alone (Fig. 5E). TUNEL analysis showed that IL-21 secretion increased cell death in tumor tissues, which consequently led to a significant decrease in Ki-67 expression (Fig. 5F−I).

3.5. *IL-21-secreting Salmonella exhibits biosafety in vivo*

Next, a series of experiments was conducted to validate the *in vivo* efficacy of *Salmonella* treatment. Initially, a BALB/c mouse model with CT26 cancer cells was used to evaluate targeting capability and biodistribution *in vivo*. Luminescent *Salmonella*-secreting IL-21 was intravenously injected when tumor size reached approximately 100−150 mm^3. The targeting capability was assessed by measuring bioluminescence intensity at 0, 2, 6, 24, 48, 72, 168, and 336 h using the IVIS Spectrum system, regardless of the L-arabinose administration. Bioluminescence signals were observed exclusively in tumors over time in mice treated with *Salmonella* (Fig. 6A and B). This result was

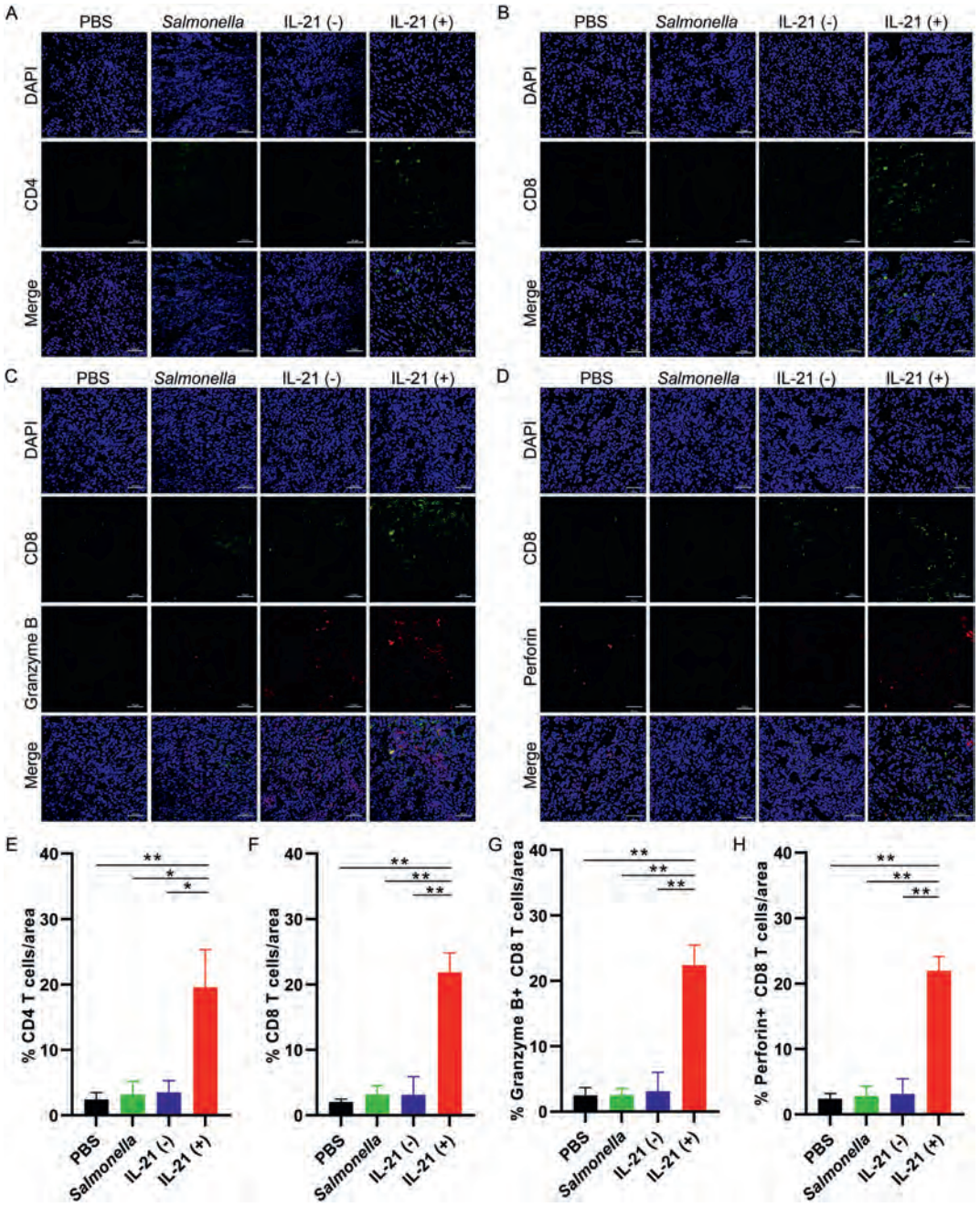

Figure 4 IL-21-secreting *Salmonella* promotes T cell infiltration and antitumor activity. The schedule for immune cell analysis is shown in Fig. 3A. (A, B) Tumor tissues obtained on Day 7 were fixed and processed for IF analysis. $CD4^+$ and $CD8^+$ T cells were analyzed using IF staining. (C, D) Granzyme B and Perforin levels in $CD8^+$ T cells were analyzed using immunofluorescence staining. Scale bar = 50 μm. Image quantification data are presented in (E−H) ($n = 3$). Significance is indicated by $^*P < 0.05$, $^{**}P < 0.01$, ns = not significant. Data are presented as the mean ± SEM.

consistent with the bioluminescence measurements of *ex vivo* organs (Supporting Information Fig. S9), suggesting that *Salmonella* specifically targets tumor tissue.

Furthermore, the targeting and biodistribution of *Salmonella* in various tissues were investigated. Tissues were collected on Days 1, 7, and 14 after injection, homogenized, and plated on Luria-Bertani (LB) agar. As shown in Fig. 6C and D, *Salmonella* primarily accumulated in the tumor over time and no *Salmonella* colonies were observed in other tissues. General biochemical markers such as BUN, CREA, ALT, and AST were also within the normal range (Fig. 6E−H). Additionally, spleen size analysis revealed transient splenomegaly compared with that in the PBS group, which returned to normal.

Histopathological examination using hematoxylin and eosin staining revealed no observable lesions (Supporting Information Figs. S10 and S11). These findings suggest that *Salmonella* does

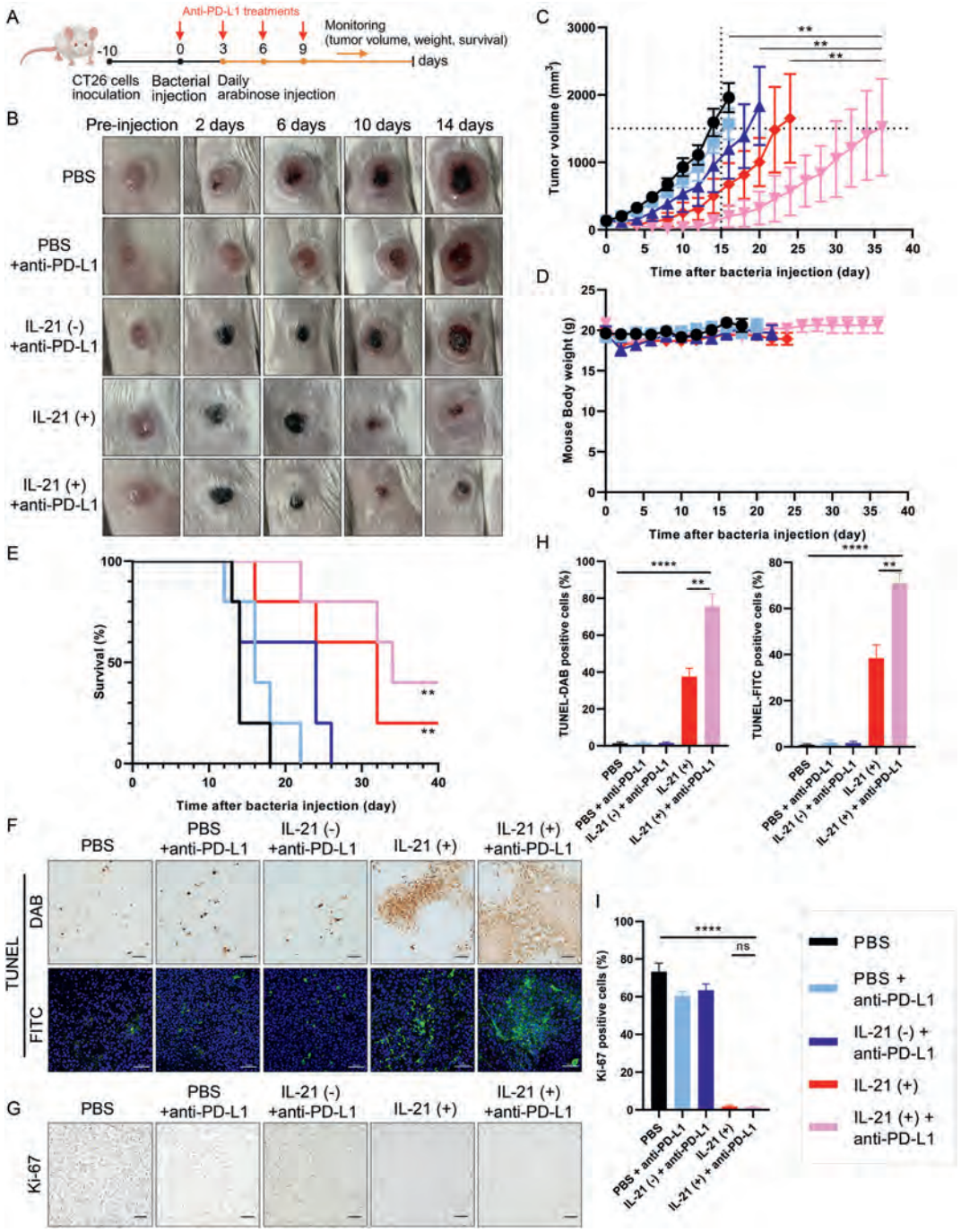

Figure 5 Antitumor efficacy of IL-21-secreting *Salmonella* combined with anti-PD-L1 antibody in tumor-bearing mice. (A) Schedule for combination therapy with IL-21-secreting *Salmonella* and anti-PD-L1 antibody. CT26 cells (5×10^5) were subcutaneously injected into the right flank of BALB/c mice. When the tumor size reached approximately 100 mm^3, *Salmonella* (2×10^7 CFU) was administered intravenously, and simultaneously, anti-PD-L1 antibody (200 μg/mouse) was administered intraperitoneally four times starting from Day 0. Additionally, starting at 3 dpi, L-arabinose (80 mg/mouse) was administered daily *via* the intraperitoneal route. IL-21(−), without L-arabinose; IL-21(+), with L-arabinose. (B) Representative images of tumor-bearing mice. (C) Tumor volume at 2-day intervals. (D) Body weight changes for each treatment group. (E) Survival curves for each treatment group (data from B−E; $n = 5$). (F) TUNEL analysis of tumors from each treatment group. (G) Ki-67 expression images of tumors from each treatment group. Scale bar = 50 μm. Image quantification data are presented in (H, I) (data from F−I; $n = 3$). Significance is indicated at $^{**}P < 0.01$, $^{****}P < 0.0001$; ns = not significant. Data are presented as the mean ± SEM.

not induce acute toxicity and can selectively and stably target tumor tissues without causing adverse effects in normal tissues. These findings highlight the potential of *Salmonella* as a safe and effective delivery system for cancer therapy with minimal toxicity

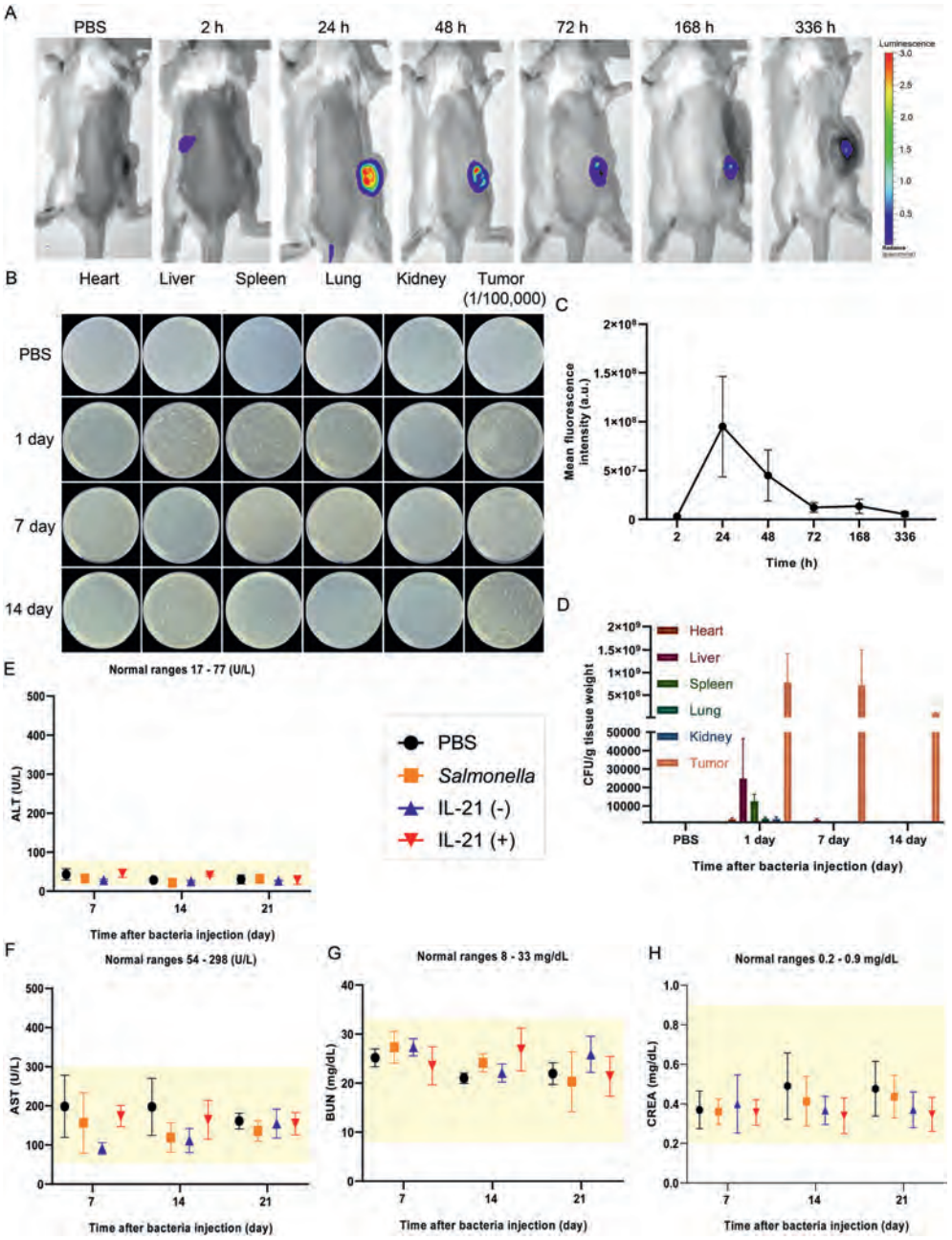

Figure 6 IL-21-secreting *Salmonella* exhibits *in vivo* biosafety. (A) IL-21-secreting *Salmonella* (2×10^7 CFU) was administered intravenously, and observations were made at 2, 24, 48, 72, 168, and 336 h. (B) After *Salmonella* administration as described in (A), tissue homogenates of the heart, liver, spleen, lung, kidney, and tumor were cultured on solid LB agar plates and photographed on Days 1, 7, and 14. (C) Time-dependent quantitative distribution of *Salmonella* in tumors and major organs in each group (data from A; $n = 3$). (D) Number of IL-21-secreting *Salmonella* clones in major organs and tumors (Data from B; $n = 3$). Data are presented as mean ± standard deviation (E−H). ALT, AST, BUN, and CREA biochemical indicators were measured in the serum at Days 7, 14 and 21 post-administrations. The yellow-shaded areas indicate the average normal range ($n = 3$). Data are presented as the mean ± SEM.

and precise tumor targeting. This indicates the possibility of inducing long-term antitumor immune responses, reinforcing its potential as a powerful tool for targeted cancer treatment.

4. Discussion

Conventional cancer treatments, such as surgery, radiation, and chemotherapy, are effective in some patients but show limited efficacy in approximately half of the patient population, necessitating the development of new therapies that directly target tumors[35]. Consequently, tumor-targeting bacteria that are capable of thriving in hypoxic environments have emerged as a promising approach for cancer treatment[36]. Bacteria can survive under hypoxic conditions, and genetically engineered bacteria, in particular, hold potential as anticancer agents by directly killing tumor cells or delivering therapeutic agents[17].

In this study, we used an attenuated *Salmonella* strain as the drug delivery platform. A tumor-targeting *Salmonella* strain was genetically engineered to secrete IL-21, which regulates immune cell interactions by tagging IL-21 with FlgM to enable its secretion through L-arabinose induction (Fig. 1A and B). Additionally, the *flhDC* gene was inserted into the plasmid to secrete IL-21 and enhance its secretion capability[19,37]. This strain targets tumors and improves the immunosuppressive tumor microenvironment, and IL-21 secreted by *Salmonella* showed antitumor effects in a tumor-bearing mouse model. In previous studies, combination therapy with *S. typhimurium* VNP20009 strain and IL-21 demonstrated antitumor effects in a tumor-bearing mouse model, along with an increase in T cell activity[25]. We used *Salmonella*, which secretes IL-21, to target tumors and enhance the activity of $CD4^+$ and $CD8^+$ T cells. Additionally, we confirmed that $CD8^+$ T cells secreted granzyme B, perforin, and IFN-γ, which are involved in their cytotoxic function (Figs. 3 and 4).

Monotherapy with IL-21 or cytokine therapy can lead to serious side effects, including systemic fevers. Although IL-21 is highly effective, it is not optimal when used alone[38,39]. However, the tumor-targeting ability of *Salmonella* can be leveraged to safely induce immunity and enhance the effects of IL-21, specifically within the tumor microenvironment, making it a promising treatment strategy (Fig. 2D).

In this study, we improved the response rate and therapeutic efficacy of PD-L1 blockade by using anti-PD-L1 antibodies in combination with IL-21-secreting *Salmonella*. Some studies have shown that approximately 20%−30% of tumor-bearing mice respond effectively to ICI therapy[40]. Additional administration of anti-PD-L1 antibodies resulted in complete tumor regression in 40% of tumor-bearing mice and improved their survival rates. This supports our findings and suggests that combination therapy with IL-21-secreting *Salmonella* and anti-PD-L1 antibodies has greater potential for cancer treatment than monotherapies. These results indicate that changes induced by *Salmonella* at the tumor site contribute to overcoming the limitations of ICI therapy. Studies have also shown that a positive response to ICIs is dependent on the extent of T cell infiltration into the tumor tissue, which suppresses immune evasion mechanisms to promote antitumor immune responses but fails to induce effective responses in certain cancers[41,42]. Preclinical studies have demonstrated that combining IL-21 with ICIs effectively amplifies immune responses and overcomes tumor immune evasion[43]. When *Salmonella* reaches the tumor site, LPS and pathogenic factors induce PD-L1 expression in tumor cells, thereby promoting immune evasion[44]. *Salmonella* plays a crucial role in enhancing the response to PD-L1 inhibitors. This is primarily achieved by increasing T cell infiltration within the tumor, directly killing the tumor cells, and releasing tumor antigens. This process can activate antigen-presenting cells, thereby stimulating T cell responses and enhancing the immune system. *Salmonella* can induce PD-L1 expression in tumors and promote immune evasion. In this context, combination therapy with anti-PD-L1 antibodies has the potential to reactivate the immune system and enhance the antitumor efficacy.

Many studies have emphasized that the use of attenuated *Salmonella* strains in cancer therapy offers the advantage of selective accumulation at tumor sites, thereby enabling the targeted delivery of therapeutic agents[45,46]. However, the safety of bacterial therapies remains a critical concern in clinical applications, necessitating strategies to control bacterial proliferation and minimize side effects in non-target areas[47]. In this study, we discovered that FlgM-tagged IL-21 was secreted *via* FT3SS, which decreased bacterial motility by reducing the expression of fliC, a gene involved in flagella formation (Fig. 1E). Temporary splenomegaly was observed until Day 7 post-infection, which returned to normal after Day 14 (Fig. S11). Hematoxylin and eosin staining revealed no significant lesions caused by strain (Fig. S10).

5. Conclusions

This study demonstrates that IL-21-secreting *Salmonella* enhances the antitumor immune responses in tumor-bearing mice, and that combination therapy with anti-PD-L1 antibodies produces synergistic effects. In particular, anti-PD-L1 therapy addresses the unmet medical needs of patients with colorectal cancer. These findings suggest the potential utilization of genetically modified bacteria in immunotherapy and establish a foundation for clinical trials aimed at optimizing combination therapies. Collectively, the integration of IL-21 secreted by genetically modified *Salmonella* with ICIs represents a promising frontier in cancer therapy, offering the potential for more effective and personalized treatment options and promoting advances in cancer immunotherapy.

Acknowledgements

We would like to thank Professor In Soo Lee for providing the *Salmonella* strains needed for the experiments. Additionally, our gratitude extends to Editage (www.editage.co.kr) for their assistance with English language editing. This work was supported by BK21 FOUR Program by Chungnam National University Research Grant, 2025. This work was also supported by National Research Foundation of Korea grants funded by the Korean government (NRF-2022R1A2C1009875 and RS-2018NR056534, Korea) and by the Korea Health Technology R&D Project through the Korea Health Industry Development Institute (KHIDI), funded by the Ministry of Health and Welfare, Republic of Korea (HR20C0025, Korea). Heung Jin Jeon was supported by NRF-RS202300243742 (Korea). Graphical abstract image was created using BioRender.

Author contributions

Minju Han, contributed to data curation, writing, review, investigation, and methodology. Eunji Kim, Minchan Jeong, and Solbi Kim, contributed to conceptualization, data curation, and investigation. Heung Jin Jeon and Hyo-Jin Lee, contributed to conceptualization, funding acquisition, review, and supervision. All authors have read and agreed to the published version of the manuscript.

Conflicts of interest

The authors declare no conflicts of interest.

Appendix A. Supporting information

Supporting information to this article can be found online at https://doi.org/10.1016/j.apsb.2025.09.025.

References

1. Anand U, Dey A, Chandel AKS, Sanyal R, Mishra A, Pandey DK, et al. Cancer chemotherapy and beyond: current status, drug candidates, associated risks and progress in targeted therapeutics. *Genes Dis* 2023;**10**:1367−401.
2. Zhong L, Li Y, Xiong L, Wang W, Wu M, Yuan T, et al. Small molecules in targeted cancer therapy: advances, challenges, and future perspectives. *Signal Transduct Targeted Ther* 2021;**6**:201.
3. Tan S, Li D, Zhu X. Cancer immunotherapy: pros, cons and beyond. *Biomed Pharmacother* 2020;**124**:109821.
4. Toor SM, Sasidharan Nair V, Decock J, Elkord E. Immune checkpoints in the tumor microenvironment. *Semin Cancer Biol* 2020;**65**:1−12.
5. Liu J, Chen Z, Li Y, Zhao W, Wu J, Zhang Z. PD-1/PD-L1 checkpoint inhibitors in tumor immunotherapy. *Front Pharmacol* 2021;**12**:731798.
6. Jia L, Zhang Q, Zhang R. PD-1/PD-L1 pathway blockade works as an effective and practical therapy for cancer immunotherapy. *Cancer Biol Med* 2018;**15**:116−23.
7. Topalian SL, Drake CG, Pardoll DM. Immune checkpoint blockade: a common denominator approach to cancer therapy. *Cancer Cell* 2015; **27**:450−61.
8. Philips GK, Atkins M. Therapeutic uses of anti-PD-1 and anti-PD-L1 antibodies. *Int Immunol* 2015;**27**:39−46.
9. McCarthy EF. The toxins of William B. Coley and the treatment of bone and soft-tissue sarcomas. *Iowa Orthop J* 2006;**26**:154−8.
10. Forbes NS. Engineering the perfect (bacterial) cancer therapy. *Nat Rev Cancer* 2010;**10**:785−94.
11. Zhou S, Gravekamp C, Bermudes D, Liu K. Tumour-targeting bacteria engineered to fight cancer. *Nat Rev Cancer* 2018;**18**:727−43.
12. Zacharski LR, Sukhatme VP. Coley's toxin revisited: immunotherapy or plasminogen activator therapy of cancer?. *J Thromb Haemostasis* 2005;**3**:424−7.
13. Kasinskas RW, Forbes NS. *Salmonella typhimurium* lacking ribose chemoreceptors localize in tumor quiescence and induce apoptosis. *Cancer Res* 2007;**67**:3201−9.
14. Heimann DM, Rosenberg SA. Continuous intravenous administration of live genetically modified *Salmonella typhimurium* in patients with metastatic melanoma. *J Immunother* 2003;**26**:179−80.
15. Saltzman DA, Katsanis E, Heise CP, Hasz DE, Vigdorovich V, Kelly SM, et al. Antitumor mechanisms of attenuated *Salmonella typhimurium* containing the gene for human interleukin-2: a novel antitumor agent?. *J Pediatr Surg* 1997;**32**:301−6.
16. Chen J, Qiao Y, Tang B, Chen G, Liu X, Yang B, et al. Modulation of *Salmonella* tumor-colonization and intratumoral anti-angiogenesis by triptolide and its mechanism. *Theranostics* 2017;**7**:2250−60.
17. Duong MT, Qin Y, You SH, Min JJ. Bacteria−cancer interactions: bacteria-based cancer therapy. *Exp Mol Med* 2019;**51**:1−15.
18. Berger E, Soldati R, Huebener N, Hohn O, Stermann A, Durmus T, et al. *Salmonella* SL7207 application is the most effective DNA vaccine delivery method for successful tumor eradication in a murine model for neuroblastoma. *Cancer Lett* 2013;**331**:167−73.
19. Singer HM, Erhardt M, Steiner AM, Zhang MM, Yoshikami D, Bulaj G, et al. Selective purification of recombinant neuroactive peptides using the flagellar type III secretion system. *mBio* 2012;**3**: e00115-12.
20. Buttner D. Protein export according to schedule: architecture, assembly, and regulation of type III secretion systems from plant- and animal-pathogenic bacteria. *Microbiol Mol Biol Rev* 2012;**76**: 262−310.
21. Sun H, Wang M, Liu Y, Wu P, Yao T, Yang W, et al. Regulation of flagellar motility and biosynthesis in enterohemorrhagic *Escherichia coli* O157:H7. *Gut Microbes* 2022;**14**:2110822.
22. Parrish-Novak J, Foster DC, Holly RD, Clegg CH. Interleukin-21 and the IL-21 receptor: novel effectors of NK and T cell responses. *J Leukoc Biol* 2002;**72**:856−63.
23. Sondergaard H, Skak K. IL-21: roles in immunopathology and cancer therapy. *Tissue Antigens* 2009;**74**:467−79.
24. Monteleone G, Pallone F, Macdonald TT. Interleukin-21 as a new therapeutic target for immune-mediated diseases. *Trends Pharmacol Sci* 2009;**30**:441−7.
25. Wang Y, Chen J, Tang B, Zhang X, Hua ZC. Systemic administration of attenuated *Salmonella typhimurium* in combination with interleukin-21 for cancer therapy. *Mol Clin Oncol* 2013;**1**:461−5.
26. Wu S, Huang H, Sun R, Gao DS, Ye F, Huang J, et al. Synergism between IL21 and anti-PD-1 combination therapy is underpinned by the coordinated reprogramming of the immune cellular network in the tumor microenvironment. *Cancer Res Commun* 2023;**3**: 1460−72.
27. Strugnell R, Dougan G, Chatfield S, Charles I, Fairweather N, Tite J, et al. Characterization of a *Salmonella typhimurium* aro vaccine strain expressing the P.69 antigen of *Bordetella pertussis*. *Infect Immun* 1992;**60**:3994−4002.
28. Datsenko KA, Wanner BL. One-step inactivation of chromosomal genes in *Escherichia coli* K-12 using PCR products. *Proc Natl Acad Sci U S A* 2000;**97**:6640−5.
29. Karlinsey JE. λ-Red genetic engineering in *Salmonella enterica* serovar Typhimurium. *Methods Enzymol* 2007;**421**:199−209.
30. Lane MC, Alteri CJ, Smith SN, Mobley HL. Expression of flagella is coincident with uropathogenic *Escherichia coli* Ascension to the upper urinary tract. *Proc Natl Acad Sci U S A* 2007;**104**:16669−74.
31. Guzman LM, Belin D, Carson MJ, Beckwith J. Tight regulation, modulation, and high-level expression by vectors containing the arabinose PBAD promoter. *J Bacteriol* 1995;**177**:4121−30.
32. Loessner H, Endmann A, Leschner S, Westphal K, Rohde M, Miloud T, et al. Remote control of tumour-targeted *Salmonella enterica* serovar Typhimurium by the use of L-arabinose as inducer of bacterial gene expression *in vivo*. *Cell Microbiol* 2007;**9**:1529−37.
33. Galan JE, Nakayama K, Curtiss R. Cloning and characterization of the asd gene of *Salmonella typhimurium*: use in stable maintenance of recombinant plasmids in *Salmonella* vaccine strains. *Gene* 1990;**94**: 29−35.
34. Daly RJ, Scott AM, Klein O, Ernst M. Enhancing therapeutic anticancer responses by combining immune checkpoint and tyrosine kinase inhibition. *Mol Cancer* 2022;**21**:189.
35. Hanahan D, Weinberg RA. Hallmarks of cancer: the next generation. *Cell* 2011;**144**:646−74.
36. Patyar S, Joshi R, Byrav DS, Prakash A, Medhi B, Das BK. Bacteria in cancer therapy: a novel experimental strategy. *J Biomed Sci* 2010;**17**: 21.
37. Guo S, Alshamy I, Hughes KT, Chevance FF. Analysis of factors that affect FlgM-dependent type III secretion for protein purification with *Salmonella enterica* serovar Typhimurium. *J Bacteriol* 2014;**196**: 2333−47.
38. Jauch D, Martin M, Schiechl G, Kesselring R, Schlitt HJ, Geissler EK, et al. Interleukin 21 controls tumour growth and tumour immunosurveillance in colitis-associated tumorigenesis in mice. *Gut* 2011;**60**: 1678−86.
39. Spolski R, Leonard WJ. Interleukin-21: a double-edged sword with therapeutic potential. *Nat Rev Drug Discov* 2014;**13**:379−95.
40. Taylor MA, Hughes AM, Walton J, Coenen-Stass AML, Magiera L, Mooney L, et al. Longitudinal immune characterization of syngeneic tumor models to enable model selection for immune oncology drug discovery. *J Immunother Cancer* 2019;**7**:328.
41. Shen S, Sckisel G, Sahoo A, Lalani A, Otter DD, Pearson J, et al. Engineered IL-21 cytokine muteins fused to anti-PD-1 antibodies can improve $CD8^+$ T cell function and anti-tumor immunity. *Front Immunol* 2020;**11**:832.
42. di Carlo E, de Totero D, Piazza T, Fabbi M, Ferrini S. Role of IL-21 in immune-regulation and tumor immunotherapy. *Cancer Immunol Immunother* 2007;**56**:1323−34.
43. Dobosz P, Stepien M, Golke A, Dzieciatkowski T. Challenges of the immunotherapy: perspectives and limitations of the immune checkpoint inhibitor treatment. *Int J Mol Sci* 2022;**23**:2847.
44. Omori Y, Noguchi K, Kitamura M, Makihara Y, Omae T, Hanawa S, et al. Bacterial lipopolysaccharide induces PD-L1 expression and an

invasive phenotype of oral squamous cell carcinoma cells. *Cancers (Basel)* 2024;**16**:343.
45. Zhang Y, Tan W, Sultonova RD, Nguyen DH, Zheng JH, You SH, et al. Synergistic cancer immunotherapy utilizing programmed *Salmonella typhimurium* secreting heterologous flagellin B conjugated to interleukin-15 proteins. *Biomaterials* 2023;**298**:122135.
46. Lin Z, Meng F, Ma Y, Zhang C, Zhang Z, Yang Z, et al. *In situ* immunomodulation of tumors with biosynthetic bacteria promote antitumor immunity. *Bioact Mater* 2024;**32**:12−27.
47. Mi Z, Feng ZC, Li C, Yang X, Ma MT, Rong PF. *Salmonella*-mediated cancer therapy: an innovative therapeutic strategy. *J Cancer* 2019;**10**: 4765−76.